Progress In Electromagnetics Research M, Vol. 110, 171–184, 2022

Ant Lion Optimization to Minimize Emissions of Power Transmission Lines

Mohammed S. H. Al Salameh* **and Sama M.-K. Alnemrawi**

Abstract—In this paper, the best arrangement of overhead transmission line conductors is determined via the ant lion optimization (ALO), to minimize the emitted electric and magnetic fields. Computed electric and magnetic fields are compared with measured data in order to confirm the validity and usefulness of the formulation. ALO algorithm is applied to optimize both single and double circuit transmission lines. The two cases of spacing between line conductors are considered, namely, taking into account the effects of ice and wind, and neglecting the effects of ice and wind. IEC-71 standards are followed for the spacings in both cases. A MATLAB computer code based on ALO algorithm is written for finding the positions of line conductors that will minimize field emissions. Significant reduction of the fields is observed owing to the new optimized positions of conductors. The optimized results of ALO are compared with previous results obtained by genetic algorithm and particle swarm optimization. To the authors' knowledge, this is the first paper that applies ALO to organize high-voltage line conductors. To demonstrate the financial applicability of the solution, comparison is held between the cost of rearranging transmission line conductors and the cost of non-reducing the fields, based on a survey for people living near high voltage line in the populated city of Irbid in Jordan. Although the operating frequency for the examples in this paper is 50 Hz, the algorithm can be used for other power frequencies such as 60 Hz. The solutions are 2D, where infinite line length is assumed. Also, the algorithm uses the recommended exposure limits of 0.4 μT for the magnetic field and 5 kV/m for the electric field.

1. INTRODUCTION

Long-term exposure to magnetic fields, at extremely low frequencies below 300 Hz, increases the risk of some diseases, such as childhood leukemia [1]. Also, harmful effects may appear on animals if they are exposed to these fields [2]. The possible negative effects of electromagnetic fields (EMFs) on the living creatures are related to the induced electric currents in their tissues, due to the interfering magnetic field [3]. Also, functional problems may occur in electrical devices due to the interfering electromagnetic fields. These electrical devices include life-supporting medical equipment such as cardiac pacemakers [4–7]. Although medical devices usually have metallic enclosures and built-in filters that can reduce EMFs interference,these measures are effective for frequencies higher than 1 kHz, which means that unfortunately these devices are not protected against low power frequencies [8].

Several methods were proposed to decrease electromagnetic fields, such as shielding [9]. However, conductive shields are not effective for reducing the magnetic field at power frequencies [10, 11]. Personal safety devices is another means to reduce low frequency electromagnetic fields [3]. Unfortunately, these devices represent extra cost and some of them were not tested if they are safe for human's health. Increasing the height of the overhead transmission line is considered as a direct method to reduce the electromagnetic fields, but this solution is not practical because of the incremental cost.

Received 6 April 2022, Accepted 17 May 2022, Scheduled 28 May 2022
* Corresponding author: Mohammed Saleh Hussein Al Salameh (salameh@just.edu.jo).
The authors are with the Department of Electrical Engineering, Jordan University of Science and Technology, Irbid 22110, Jordan.

Another method involves decreasing the spacing between the phases of a transmission line, but this method has many serious disadvantages such as, radio interference and corona losses due to increased voltage gradient [12]. Electromagnetic fields were also reduced by arranging the phase-sequence of the transmission line [13, 14]. The electric and magnetic fields generated by overhead transmission lines were minimized by applying optimal phase arrangement technique [15]. A well-known arrangement for double circuit line that reduces electromagnetic fields is the negative phase sequence ABC/CBA. This method has the advantage that phase interchanging between the substation and the tower can be easily done in the control box at the substation. It is possible to minimize the fields by arranging the positions of line conductors using intelligent optimization techniques, e.g., particle swarm optimization (PSO) [16], and genetic algorithm optimization (GAO) [17, 18]. PSO algorithm was utilized to minimize only the magnetic field of high voltage lines [19]. Also, PSO algorithm was used to minimize the electric and magnetic fields of high voltage lines [20]. Also, GAO algorithm was used to minimize the electromagnetic fields of high voltage lines [21]. Differential evolution method was used to minimize the tower height without increasing the magnetic and electric fields of the line [22]. Differential evolution method was also used to minimize the electric fields at ground level of high surge impedance loading transmission lines [23]. For further information on optimization for minimizing magnetic fields of power system, the reader is referred to the review paper [24].

To the authors' knowledge, this is the first paper that uses the ant lion optimization (ALO) technique to minimize the electric and magnetic fields of high voltage transmission line. ALO, which is based on an intelligent mechanism, works in the same way that antlions use for hunting in nature by five sequential steps: ants walk in a random way, antlion makes trap, ant is entrapped, antlion catches the prey, and antlion makes new trap [25].

The authors claim the following principal contributions: new application of ALO algorithm to solve the engineering problem of optimizing high voltage transmission lines in order to minimize emanated EMFs, detailed description of all steps and equations necessary to apply ALO to high voltage transmission lines, and viability study which considers both installation costs and possible health impact costs, in the case that the line passes through populated area. The proposed model is able to optimize single as well as double circuit transmission lines, single or bundled conductors, various transmission line configurations, and for different constraints such as wind and ice or no wind and ice conditions. The algorithm is verified by comparison with measurements and with other optimization techniques which were previously applied to high voltage lines. Thus, ALO is an alternative method to other optimization methods.

2. ALO ALGORITHM

ALO is a natural inspired algorithm; it has the intelligent behavior of antlions hunting mechanism in nature. This mechanism mimics the interaction between antlions and ants, which includes the five steps mentioned above. In this paper, ants represent the random positions of the conductors of the transmission line, and the trap represents the best position of the conductors, that minimizes electric and magnetic fields. The random walk of each ant is represented by [25]:

$$X(t) = [0, cumsum\left(2r\left(t_1\right)-1\right), cumsum\left(2r\left(t_2\right)-1\right), \ldots, cumsum\left(2r\left(t_n\right)-1\right)] \tag{1}$$

$$r\left(t_i\right) = \begin{cases} 1, & If\ rand < 0.5 \\ 0, & If\ rand \geq 0.5 \end{cases}$$

where $cumsum$ is the cumulative summation of the positions of the variable on the x or y axis, $r(t_i)$ the moving factor, n the maximum number of iterations, and $rand$ the random number uniformly generated in the interval [0, 1]. Then, the positions of the ants are saved in a matrix. The position of an ant is updated at each iteration according to Equation (1). Of course, ant position should not exceed the limits. These limits are defined by this formula [25]:

$$X_{i(new)}^t = \frac{\left(X_i^t - a_i\right) \times \left(d_i - c_i^t\right)}{\left(d_i^t - a_i\right)} + c_i^t \tag{2}$$

where $X_{i(new)}^t$ is the updated position of i-th variable at iteration t, X_i^t the position of the i-th variable at iteration t, a_i the minimum random walk for the i-th variable, b_i the maximum random walk for i-th

variable, c_i^t the minimum random walk of i-th variable at iteration t, and d_i^t the maximum random walk of i-th variable at iteration t. Equation (2) is applied in each iteration to restrict the random walk in the search space.

The antlions' traps will affect the random walk of the ants and this could be modeled by:

$$c_i^t = Antlion_j^t + c^t, \quad d_i^t = Antlion_j^t + d^t \tag{3}$$

where c^t is the minimum random walk for all variables at t-iteration, d^t the maximum random walk for all variables at t-iteration, and $Antlion_j^t$ the position of j-th antlion at the t-iteration. According to (2) and (3), the ants randomly walk in a hyper sphere by the vectors c and d around a selected antlion. Then, sliding ants towards antlion is described by:

$$c^t = c^t/I, \quad d^t = d^t/I, \quad I = 10^w \frac{t}{T} \tag{4}$$

Case1: $w = 2$ when $t > 0.1\,\mathrm{T}$,
Case2: $w = 3$ when $t > 0.5\,\mathrm{T}$,
Case3: $w = 4$ when $t > 0.75\,\mathrm{T}$,
Case4: $w = 5$ when $t > 0.9\,\mathrm{T}$,
Case5: $w = 6$ when $t > 0.95\,\mathrm{T}$.

where T is the maximum iteration, and w is the constant based on the current iteration which adjusts the level of exploitation. Formula (4) decreases and shrinks the radius of the new ant's position. The final stage is catching prey and re-building the pit; this happens when an ant is caught by antlions jaw:

$$Antlion_j^t = Ant_i^t \tag{5}$$

where Ant_i^t is the position of the i-th ant at t-iteration. Note that when ants become fitter than its corresponding antlion, (5) updates the position of the corresponding antlion. The fitness position is the target. So, the antlion is the point which reduces the electric and magnetic fields.

The target of applying the algorithm is to find the best positions for the transmission line conductors that reduce both electric and magnetic fields. The solution space is limited by boundaries to make sure that the conductors' positions are within the permitted region. Two cases of clearances are considered: without ice and wind effects and with ice and wind effects according to IEC-71 standards [26]. So, the following limitations are applied:

a. Height of the lowest conductor should not be less than the minimum height: $y_{lowest\ conductor} \geq h_{\min}$.
b. Height of the highest conductor should not exceed the maximum height: $y_{highest\ conductor} \leq h_{\max}$.
c. Location of the conductor farthest from the tower should not exceed the maximum distance: $x_{farthest\ conductor} \leq D_{\max}$.
d. Location of the conductor closest to the tower should not be less than the minimum distance: $x_{closest\ conductor} \geq D_{\min}$.
e. Spacing between the conductors shouldn't be less than the minimum allowed:

$$\sqrt{(x_{cond\_i} - x_{cond\_j})^2 + (y_{cond\_i} - y_{cond\_j})^2} \geq S_{min\ spacing} \tag{6}$$

In the algorithm used in this paper, maximum number of iterations is 1000. As the recommended exposure limits are $0.4\,\mu\mathrm{T}$ for the magnetic field [5], and $5\,\mathrm{kV/m}$ for the electric field, the following objective function is used:

$$Objective\ function = \mathrm{Min}\left(B + E \times \left(8 \times 10^{-11}\right)\right) \tag{7}$$

where B is the magnetic flux density, and E is the electric field. This formula will ensure that both the electric field and magnetic field are minimized at the same time. If the value of the fitness function, of the positions of conductors at t-th iteration, is below the previous best value, the best positions of conductors will be replaced by the new positions of the t-th iteration, and the best value will also be updated.

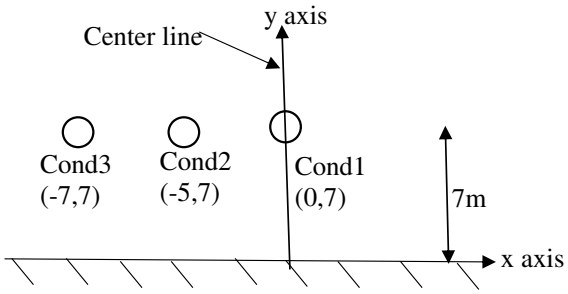

Figure 1. Cross section of three-phase line before optimization.

For simplicity, the three-phase single circuit line shown in Fig. 1 is used to explain ALO solution algorithm. For each conductor, there are two variables x and y, so we have six variables in this problem. The number of variables is equal to the number of ants in ALO, so we have six ants. Ants' positions are initialized by the positions of conductors before optimization. Also, upper and the lower limits for each variable are specified, where a_i, b_i are minimum and maximum random walk for the i-th variable. Referring to Fig. 1, for cond1 the limits are chosen as: $a_{x1} = -0.55$, $a_{y1} = 21$, $b_{x1} = 3.5$, $b_{y1} = 27.4$. Set maximum iterations Max_iter = 1000. Initialize the objective value: Objective value = $0.8\,\mu$T. The spacing conditions should be satisfied in each iteration, such as minimum phase-to-phase spacing $= 1.1$ m, i.e., For cond1 $(x_1,\ y_1)$ and cond2 $(x_2,\ y_2)$: $\sqrt{(x_1 - x_2)^2 + (y_1 - y_2)^2} \geq 1.1$. After the first iteration, the obtained new positions of the conductors are: Cond1 $(-4.5, 27.4)$, Cond2 $(-6.6, 21.14)$, Cond3 $(-3, 24.4)$. These positions give the first iteration best values, so we initialize the antlions by these positions, where $E_{\max} = 0.454\,$kV/m, $B_{\max} = 0.6383\,\mu$T. At iteration 1000: Cond1 $(-2.9, 23.4)$, Cond2 $(-2.72, 21.1)$, Cond3 $(-3.4, 22.5)$, $E_{\max} = 0.229\,$kV/m and $B_{\max} = 0.2179\,\mu$T. We can see that these results satisfy the objective values where $B_{\max} < 0.4\,\mu$T and $E_{\max} < 5\,$kV/m.

3. ELECTRIC AND MAGNETIC FIELDS

This section illustrates the formulation used to calculate the magnetic field and electric field generated by a transmission line.

3.1. Magnetic Field

For overhead transmission line, the total magnetic field is calculated by superimposing the field of each conductor, while taking into account the earth return currents. The expression of total magnetic field [27] at the point (x, y), due to N number of phase conductors parallel to the z-axis located at points (x_i, y_i) where i assumes the values $1, 2, 3, \ldots, N$, is:

$$\vec{H}\,(x,y) = \sum\nolimits_{i=1}^{i=N} \frac{I_i}{2\pi r_i}\hat{u}_i - \sum\nolimits_{i=1}^{i=N} \frac{I_i}{2\pi \grave{r}_i}\left(1 + \frac{1}{3}\left(\frac{2}{\gamma \grave{r}_i}\right)^4\right)\hat{u'}_i \tag{8}$$

$$r_i = \sqrt{(x - x_i)^2 + (y - y_i)^2}, \quad \grave{r}_i = \sqrt{(x - x_i)^2 + \left(y + y_i + \frac{2}{\gamma}\right)^2}, \quad \gamma = \sqrt{j\omega\mu(\sigma + j\omega\varepsilon)}$$

$$\hat{u}_i = \frac{y_i - y}{r_i}\hat{u}_x - \frac{x_i - x}{r_i}\hat{u}_y, \quad \hat{u'}_i = \frac{y + y_i + {}^{2}\!/_{\gamma}}{\grave{r}_i}\hat{u}_x - \frac{x_i - x}{\grave{r}_i}\hat{u}_y$$

where I_i is the electric current in each phase; $\hat{u}_x$ is the unit vector along x-axis; $\hat{u}_y$ is the unit vector along y-axis; σ, μ are electric conductivity and magnetic permeability of earth; and ω is the angular frequency. The magnetic flux density is given by: $\vec{B} = \mu_0\vec{H}$ where $\mu_0 = 4\pi \times 10^{-7}\,$H/m is the magnetic permeability of free space.

3.2. Electric Field

Electric field around a transmission line can be calculated by representing earth effect using image charges located under the earth at depth similar to the corresponding conductor height. The total electric field at point (x, y) due to N number of phase conductors parallel to the z-axis located at points (x_i, y_i) where i assumes the values $1, 2, 3, \ldots, N$, is:

$$\vec{E}(x,y) = \sum_{i=1}^{i=N} \frac{q_i}{4\pi\varepsilon_0} \left[\frac{2(y-y_i)\hat{u}_y + 2(x-x_i)\hat{u}_x}{(y-y_i)^2 + (x-x_i)^2} - \frac{2(y+y_i)\hat{u}_y + 2(x-x_i)\hat{u}_x}{(y+y_i)^2 + (x-x_i)^2} \right] \tag{9}$$

$$q_i = C_i V_i, \quad C_i = \frac{0.0556}{\ln\left(\frac{GMD}{r_i}\right)}, \quad GMD = \sqrt[3]{D_{12}D_{23}D_{13}}$$

where $\varepsilon_0 = \frac{10^{-9}}{36\pi}$ F/m is the permittivity of free space, q_i the electric line charge, V_i the phase voltage, C_i the phase capacitance in μF/km, GMD the geometric mean distance, i.e., equivalent conductor spacing, r_i the conductor radius, and D_{12} the distance between conductors 1 and 2. For bundles arrangement of phase conductors [28]: $r_i = \sqrt[n]{r \times d^{(n-1)}}$ where n is number of sub-conductor bundles, and d is bundle spacing, and r is bundle conductor radius.

For double circuit transmission lines, the formula of the capacitance is written as:

$$C_i = \frac{0.0556}{\ln \frac{GMD}{GMR_c}} \text{ μF/km} \tag{10}$$

$$GMR_C = \sqrt[3]{r_A r_B r_C}, \quad GMD = \sqrt[3]{D_{AB}D_{BC}D_{AC}}$$

$$r_A = \sqrt{r_a^b D_{a1a2}}, \quad r_B = \sqrt{r_b^b D_{b1b2}} \quad \text{and} \quad r_C = \sqrt{r_c^b D_{c1c2}}$$

$$D_{AB} = \sqrt[4]{D_{a1b1}D_{a1b2}D_{a2b1}D_{a2b2}}, \quad D_{BC} = \sqrt[4]{D_{b1c1}D_{b1c2}D_{b2c1}D_{b2c2}},$$

$$D_{AC} = \sqrt[4]{D_{a1c1}D_{a1c2}D_{a2c1}D_{a2c2}}$$

where r_i^b is the geometric mean radius of bundled conductors of phase i; D_{i1i2} is the distance between phase i in circuit 1 and phase i in circuit 2, where $i = a$ or b or c; D_{a1b1} is the distance between phase a and phase b in circuit 1; D_{a1b2} is the distance between phase a in circuit 1 and phase b in circuit 2 as illustrated in Fig. 2 in which $a1$, $b1$, $c1$ are phases of circuit 1 while $a2$, $b2$, $c2$ are phases of circuit 2.

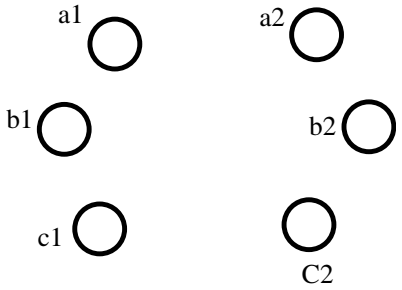

Figure 2. Cross section of double circuit transmission line phase conductors.

4. RESULTS

In this section, both electric and magnetic fields are compared with measured data. In addition, ALO optimized solutions are compared with PSO solutions available in [20]. ALO solutions are also compared with genetic algorithm optimization (GAO) solutions available in [29]. Note that it is not expected to obtain identical solutions when using ALO, PSO and GAO. These dissimilar solutions could be attributed to the fact that these methods are different because they are based on different

biological phenomena. The electric and magnetic fields are given for the transmission line before and after optimization where significant reduction is obtained. Two types of transmission lines are studied: single-circuit transmission lines, and double circuit transmission lines. The execution time of the MATLAB program for ALO is less than 7 seconds when it is run on a computer that has the specifications: HP, Intel(R) Corei3(TM)i3-1005G1CPU@1.20 GHz, RAM 4 GB.

4.1. Verification of Electric Field Formulation

The electric field equations of Section 3 above will be used through the ALO optimization. To verify these equations, the electric field of an existing transmission line illustrated in Fig. 3 is calculated and compared with measured data, where results agree well with each other as can be seen in Fig. 4. The field is evaluated at 1 m above ground, under the transmission line. The small differences between the measured and calculated values may be partly attributed to the varying voltage with time during measurements.

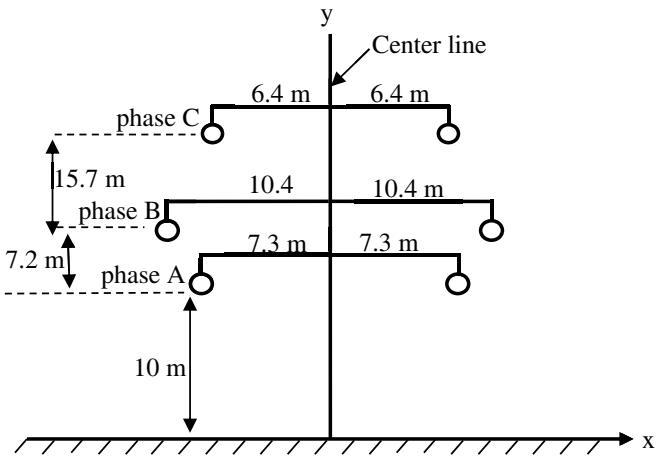

Figure 3. Cross section of double circuit 400 kV high voltage transmission line.

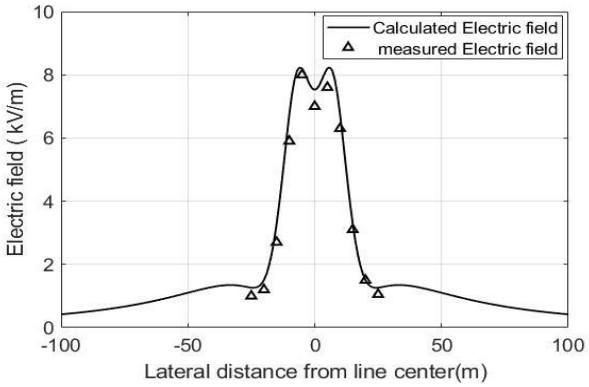

Figure 4. Calculated electric field as compared with measured electric field [30] under double circuit 400 kV line at 1m above ground, i.e., $y = 1$ m.

4.2. Verification of Magnetic Field Formulation

The magnetic field, of the double circuit 132 kV parentheses transmission line shown in Fig. 5, is calculated at 1 m above ground. The arrangement of the phases A, B, C is the same in both circuits. During measurements, the electric current in each phase on the left circuit was 91 A, while on the right

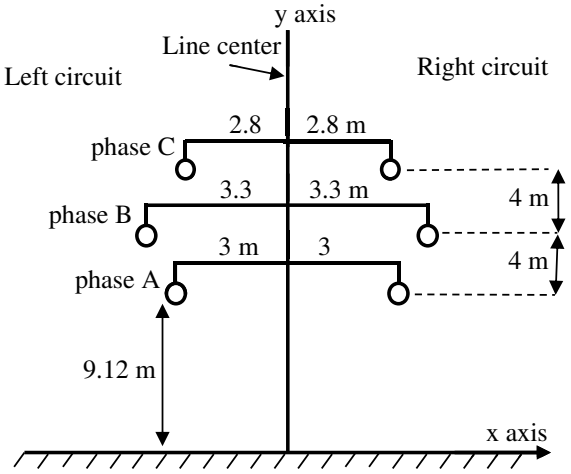

Figure 5. Existing double circuit 132 kV parentheses transmission line.

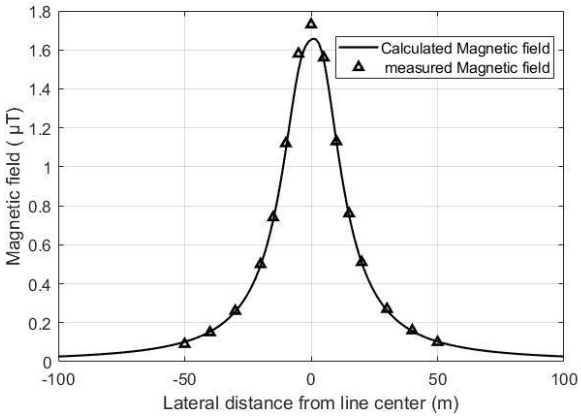

Figure 6. Calculated vs. measured magnetic flux density under the double circuit 132 kV parentheses line.

circuit it was 104 A [27]. The results shown in Fig. 6 reveal good agreement between computed and measured data.

4.3. Single Circuit 132 kV Vertical Transmission Line

The vertical 132 kV line has three conductors, as shown in Fig. 7. The mean current in the three phases is 320 A, with a little bit of unbalance between phases: 338 A in phase A, 312 A in phase B, and 310 A in phase C [27]. The calculated and measured magnetic flux densities are plotted in Fig. 8 where acceptable agreement is readily seen.

The magnetic flux densities before and after ALO optimization are shown in Fig. 9, where ALO solutions are compared with PSO and GAO solutions for the single circuit 132 kV vertical line with ice and wind effects. In this figure, peak value of the magnetic flux density of the existing line before optimization is 0.9 μT at 1 m height above the ground and ROW = 55 m, compared with peak value of 0.6 μT and ROW = 34 m after ALO optimization. Using PSO, peak value of 0.58 μT and ROW = 32 m are obtained. Using GAO, peak value of.76 μT and ROW = 44 m are obtained. These results along with Fig. 9 show that ALO and PSO results are close to each other, and both are better than GAO results.

Now, without ice and wind effects, magnetic flux densities before and after ALO optimization are shown in Fig. 10, where ALO solutions are compared with PSO solutions for the single circuit 132 kV

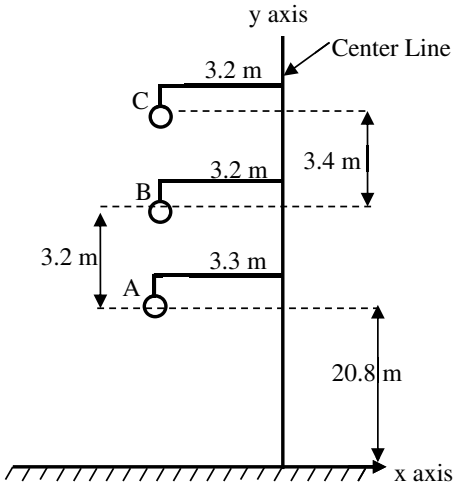

Figure 7. Existing single circuit 132 kV vertical transmission line.

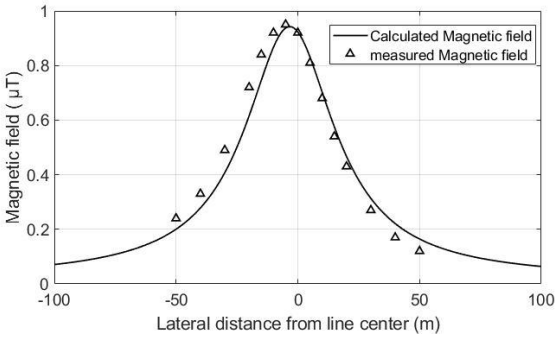

Figure 8. Calculated and measured magnetic flux densities vs. location from line center for the single circuit 132 kV vertical configuration.

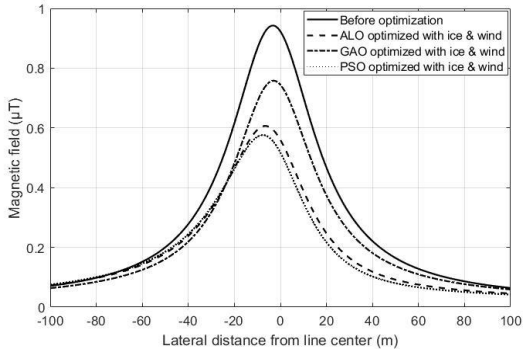

Figure 9. Magnetic flux densities, with ice and wind effects, under the 132 kV vertical line at $y = 1$ m before and after ALO, PSO, and GAO optimizations.

vertical line. In this figure, peak value of the magnetic flux density is 0.22 μT and ROW = 0 m after ALO optimization. Using PSO, peak value of about 0.2 μT and ROW = 0 m are obtained. Again, ALO and PSO results are close to each other.

The electric field is calculated at different lateral distances from the line as shown in Fig. 11 for the line with ice and wind effects, both before and after ALO, PSO, GAO optimizations. The electric field peak value for the existing line without optimization is 0.47 kV/m, compared with the peak value of 0.36 kV/m after ALO optimization. After PSO optimization, peak electric field is 0.22 kV/m, and after GAO optimization, peak value is 0.38 kV/m. Here, ALO and GAO are close to each other, while PSO is better than both of them.

The calculated electric field is shown in Fig. 12 for the same line without ice and wind effects, both before and after ALO and PSO optimizations. The peak value of electric field after ALO optimization is 0.23 kV/m, whereas peak value using PSO is 0.22 kV/m. Thus, both techniques reach almost the same minimized electric field.

Positions of the conductors of the existing 132 kV vertical line before optimization in addition to the positions of the conductors after ALO, PSO, GAO optimizations are illustrated in Fig. 13, where it is clear that different optimization techniques produce different optimized configurations and consequently different field values.

The convergence of the ALO algorithm, for this example without ice and wind effects, is shown in

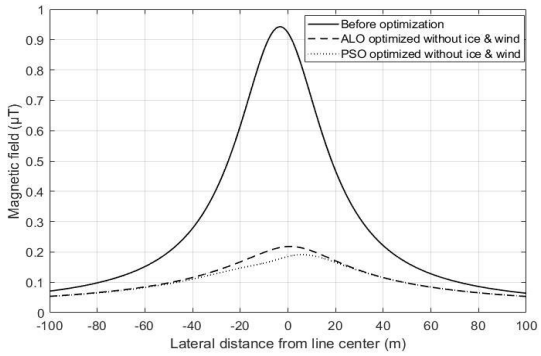

Figure 10. Magnetic flux densities, without ice and wind effects, under the 132 kV vertical line at $y = 1$ m before and after ALO and PSO optimizations.

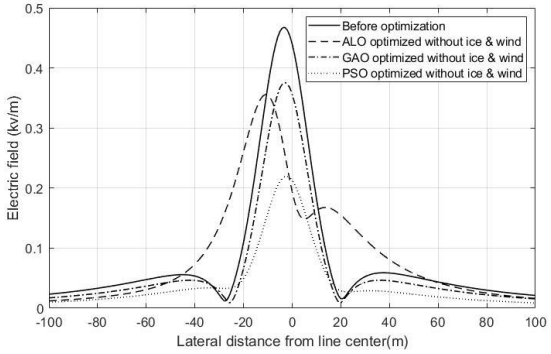

Figure 11. Electric field under the single circuit 132 kV vertical line at $y = 1$ m, with ice and wind effects.

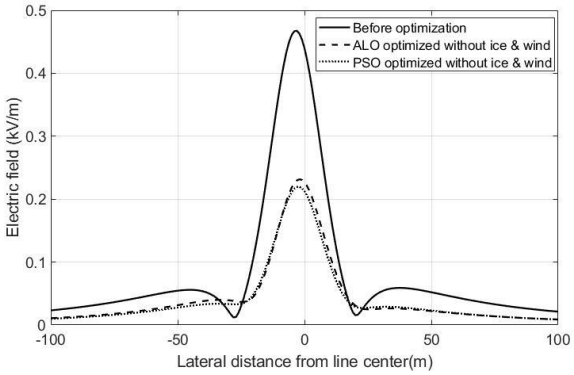

Figure 12. Electric field profile under the single circuit 132 kV line, at $y = 1$ m.

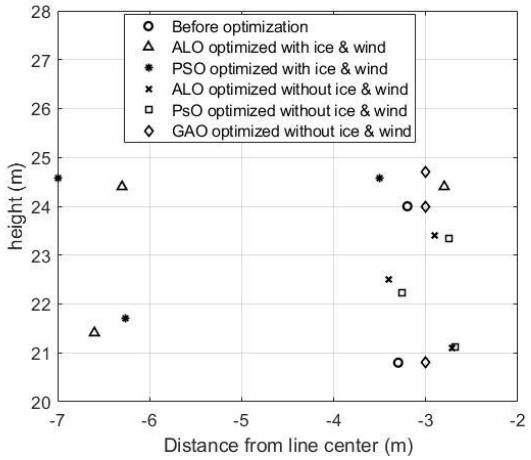

Figure 13. Positions of conductors before and after ALO, PSO, GAO optimizations.

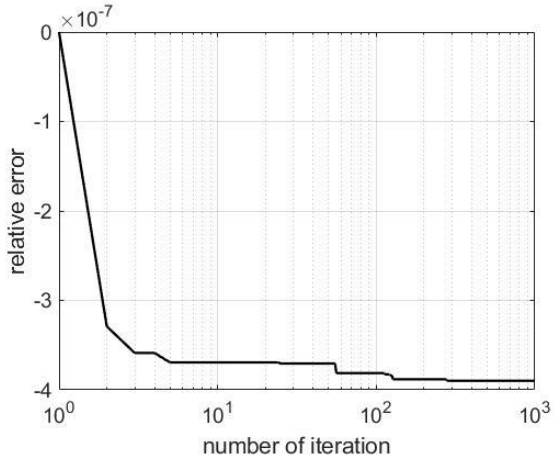

Figure 14. Convergence of the relative error with iterations using ALO.

Fig. 14 where the relative error is the difference between the best obtained value at each iteration and the objective value: $Relative\ error = \frac{Best\ value - Objective\ value}{Objective\ value}$. For this example, the error saturates after 300 iterations, as can be seen in Fig. 14. Note that relative error is negative since best obtained

value is lower than the objective value for the 132 kV vertical line as shown in Fig. 10. We have tried several examples and found that the solution converges after several hundreds of iterations. Based on that, maximum number of iterations chosen is 1000.

4.4. Double Circuit 230 kV Delta Line

Each conductor in this circuit consists of two bundles, where the spacing between the bundles is 18 inches, and the current in each phase is 740 A [27]. The configuration of this circuit is shown in Fig. 15.

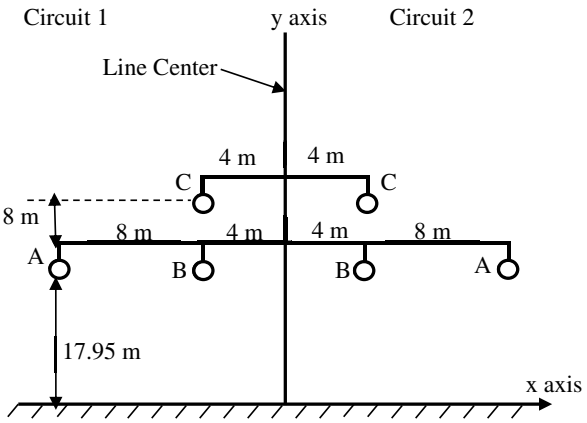

Figure 15. Cross section of the double circuit 230 kV delta line.

The magnetic flux densities, for the existing line before optimization and after ALO optimization, are shown in Fig. 16. The two cases are considered: with ice and wind effects, and without ice and wind effects. The peak value of the magnetic flux density before optimization is 4.9 μT and ROW = 148 m, while peak value after applying ALO with ice and wind effects is 1.3 μT and ROW = 80 m. Without ice and wind effects, ALO peak value is 0.38 μT and ROW = 0 m.

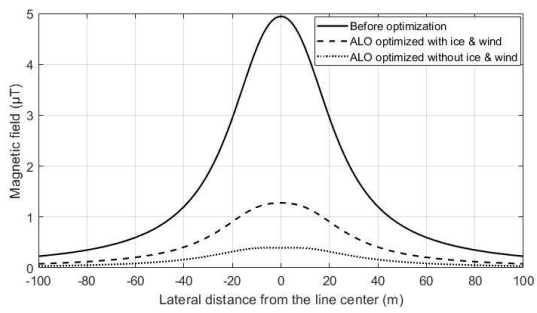

Figure 16. Magnetic flux density under the double circuit 230 kV delta line at $y = 1$ m.

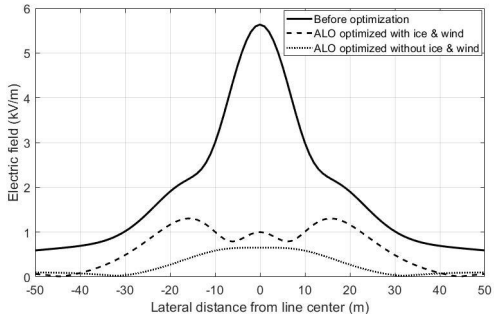

Figure 17. Electric field under the double circuit 230 kV delta line at $y = 1$ m.

Electric fields, for the existing line before optimization and after ALO optimization, are shown in Fig. 17. The peak value of the electric field before optimization is 5.6 kV/m, while peak value after applying ALO with ice and wind effects is 1.3 kV/m. Without ice and wind effects, ALO peak value is 0.65 kV/m.

The positions of the conductors before and after optimization are shown in Fig. 18. In Fig. 18, phase to phase distance after optimization is 6.2 m for the case of ice and wind, whereas it is 2.4 m in case ice and wind are neglected. According to IEC-71 standards, minimum phase-phase clearance is 6 m for the case of ice and wind, whereas it is 2.4 m in case ice and wind are neglected. So, the optimized solutions comply with the IEC-71 standards.

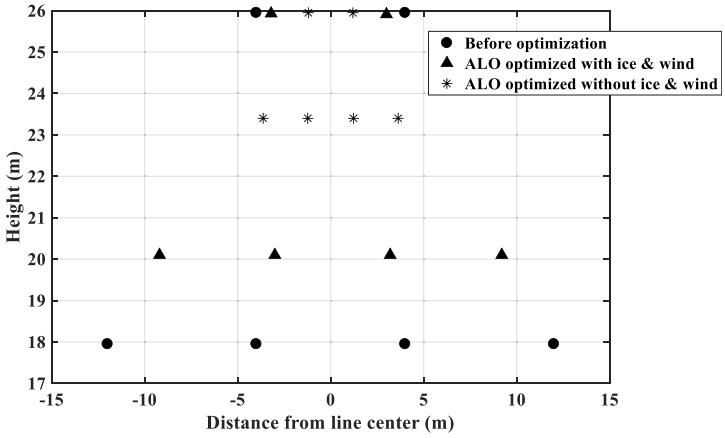

Figure 18. Positions of conductors of the double circuit 230 kV delta line before and after ALO optimization.

5. FINANCIAL COST DISCUSSION

The algorithm described in this paper is intended to be used for new transmission lines. Thus, there are no additional costs associated with conductor arrangement since conductors' positions are determined in the design stage before installing the line. However, should the need arise for rearranging the conductors of an existing transmission line, the following viability case study favors the rearrangement. The positions of the conductors of high voltage transmission line are optimized in order to minimize the magnetic and electric fields associated with the line, in an attempt to keep away the possible negative health effects on exposed people living nearby. Not only that, but also decreasing the fields reduces the opportunity of interference with nearby electronic and electrical devices and furthermore reduces possible ecological adverse effects of these emissions. Although the issue of negative health impacts is controversial, the precautionary principle dictates protective action when the scientific evidence related to the risk is not complete. In order to check the viability of rearranging the line conductors to decrease the emissions, the financial cost of repositioning the conductors of a transmission line is compared with the financial cost of potential diseases and fatalities related to the higher fields. Therefore, we performed a case study on a 3 km segment of the 132 kV transmission line passing through the city of Irbid in Jordan, as shown in Fig. 19, where some inhabited houses are very close and even directly under the high voltage transmission line. The goal is to approximately find the number of people residing within 100 m on either side of the line, where the residential units considered were 2000. To calculate the

Figure 19. View of the study area in Irbid, Jordan.

total number of individuals in the study area, we need the average number of individuals per family in Jordan which is 5.3 as given by the Jordanian Department of Statistics. Accordingly, the overall number of humans, residing within 100 m on either side of the 3 km portion of the transmission line, is calculated by the product of these two numbers (2000×5.3) which amounts to 10,600 persons. Using the predictions given in [31], deaths are estimated to be 16 in addition to 80 cases of illness each year amongst the 10,600 humans living in close proximity to the high voltage line, linked with long-term exposure to magnetic and electric emissions. On the other hand, if the positions of the conductors of high voltage transmission line are rearranged in order to minimize the magnetic and electric fields, population exposure will decrease, and consequently the expected illnesses and fatalities will decline. The expected deaths and illnesses after rearranging the line are estimated to be 10 and 50, respectively, based on the calculated reduction of ROW from 55 m to 34 m in the ALO optimized 132 kV transmission line example given above. In view of that, 6 ($= 16-10$) fatalities and 30 ($= 80-50$) illnesses are expected to be avoided every year within the study zone.

The value of statistical life "VSL" for preventing risks of electromagnetic fields in USA was estimated in 1998 to be \$5 million per death, and the value of illness "VOI" was estimated to be \$0.2 million per non-fatal illness [31, 32]. The values of VSL and VOI can be assessed for Jordan using Equation (1) in [33], using the fact that the gross domestic product (GDP) per capita in 1998 in USA was \$32,853.677 while in Jordan it was only \$1600.398. Accordingly, in 1998, VSL in Jordan is expected to be \$243,565 and VOI = \$48, 713. To modify VSL for future years, the change in VSL is the same as the change in income which is estimated to be 0.8% increase per year [34]. Thus, for Jordan in 2022, VSL is estimated to be \$294,895 and VOI = \$58, 979. Assuming that rearrangement of the transmission line will be realized in 2023, then by the end of the year 2052, as the average lifetime of overhead transmission lines is 30 years, VSL will be \$374,527 and VOI = \$74, 905. Using an annual profit rate of 4%, the present value in 2023 of these VSL and VOI are \$115,474 and \$23,095, respectively. In accordance with that, the net present value of the estimated financial costs for deaths and illnesses attributed to nondecreasing the transmission line emissions within the lifetime of the line (30 years) reaches \$67.8 million.

On the other hand, the cost, to reduce electromagnetic fields from high voltage transmission line by using different arrangement of conductors, was estimated as \$90,000/mile in 1994 [35]. This rearrangement cost can be estimated for Jordan by comparing GDP per capita of Jordan and USA in 1994. The GDP per capita in 1994 was \$27,694.853 in USA while it was only \$1,414.339 in Jordan. Therefore, the cost to rearrange the conductors is estimated to be \$4,596/mile in Jordan in 1994. Using the annual inflation rates in Jordan for the years 1995–2023 [36], the cost of rearranging a mile of the line in 2023 would be \$10,785. Arranging the 3 km segment of the transmission line will cost around \$20,104 in 2023. In brief, arranging the 3 km segment of the line will cost only \$20,104 compared to \$67.8 million for fatalities and illnesses due to nonreducing the EM fields. This comparison supports the idea of rearranging the transmission line.

6. CONCLUSIONS

This study aimed at using the ALO algorithm to find the best arrangement of the transmission line conductors, that minimizes the electric and magnetic fields. Towards that end, computer code is written using MATLAB to apply ALO. The results presented in this paper show that ALO is successfully applied to minimize the fields. The solutions obtained using ALO are compared with results of PSO and GAO. Some examples show that ALO outperforms PSO and GAO, whereas other examples show that ALO underperforms PSO and GAO. Many configurations were used including single circuit and double circuit transmission lines. In order to show the validity and applicability of the solutions, calculated results are compared with measured data where agreement is observed. Solutions are given for the two conditions of lines: without ice and wind effects,and with ice and wind effects. Case study for an inhabited area in close proximity to a high voltage transmission line is presented where the financial cost analysis is in favor of rearranging the line in order to reduce long term exposure to the line emissions.

ALO algorithm is able to find designs for the engineering problem of optimizing the high voltage transmission line configuration in order to reduce the possible ecological impact of the associated electromagnetic fields, showing that ALO has merits in solving constrained problems with diverse search

spaces. In addition, the use of random walks has the potential to overcome local optima stagnation. Ants' movements are progressively decreased throughout iterations, which guarantees convergence of the algorithm. ALO algorithm is simple and has few parameters to tune. However, ALO algorithm has some limitations, such as limited accuracy in some examples presented in this paper, where ALO was outperformed by other optimization techniques. Future research, related to high voltage lines, will be conducted to enhance the performance of the algorithm.

REFERENCES

1. Bonato, M., et al., "Characterization of children's exposure to extremely low frequency magnetic fields by stochastic modeling," *Int. J. Environ. Res. Public Health*, Vol. 15, No. 9, 1963, 2018.
2. Baharara, J. and Z. Zahedifar, "The effect of low-frequency electromagnetic fields on some biological activities of animals," *Arak Med. Univ. J.*, Vol. 15, No. 7, 2012.
3. Florea, G. A., A. Dinca, and S. I. A. Gal, "An original approach to the biological impact of the low frequency electromagnetic fields and proofed means of mitigation," *2009 IEEE Bucharest PowerTech*, 1–8, 2009.
4. Townsend, D. A., "Risk analysis and EMI risk abatement strategies for hospitals: Scientific and legal approaches," *IEEE International Symposium on Electromagnetic Compatibility*, Vol. 2, 1304–1307, 2001.
5. Maisch, D., J. Podd, and B. Rapley, "Changes in health status in a group of CFS patients following removal of excessive 50 Hz magnetic field exposure," *Journal of Australian College of Nutritional & Environmental Medicine*, Vol. 21, No. 1, 15–19, Apr. 2002.
6. Dawson, T. W., K. Caputa, M. A. Stuchly, R. B. Shepard, R. Kavet, and A. Sastre, "Pacemaker interference by magnetic fields at power line frequencies," *IEEE Trans. Biomed. Eng.*, Vol. 49, No. 3, 254–262, 2002.
7. Yerra, L. and P. C. Reddy, "Effects of electromagnetic interference on implanted cardiac devices and their management," *Cardiology in Review*, Vol. 15, No. 6, 304–309, 2007.
8. Smith, S. and R. Aasen, "The effects of electromagnetic fields on cardiac pacemakers," *IEEE Trans. Broadcast.*, Vol. 38, No. 2, 136–139, 1992.
9. Zhu, Y., C. Gao, L. Shi, and B. Zhou, "Analysis and test of EM shielding for low-frequency magnetic field," *IEEE International Symposium on Electromagnetic Compatibility*, 345–349, Qingdao, China, Oct. 23–26, 2007.
10. Wassef, K., V. V. Varadan, and V. K. Varadan, "Magnetic field shielding concepts for power transmission lines," *IEEE Transactions on Magnetics*, Vol. 34, No. 3, 649–654, 1998.
11. Canova, A. and L. Giaccone, "Magnetic field mitigation of power cable by high magnetic coupling passive loop," *IET Conference Publications*, No. 550, CP, 2009.
12. Melo, M. O. B. C., L. C. A. Fonseca, E. Fontana, and S. R. Naidu, "Electric and magnetic fields of compact transmission lines," *IEEE Transactions on Power Delivery*, Vol. 14, No. 1, 200–204, 1999.
13. Filippopoulos, G., D. Tsanakas, G. Kouvarakis, J. Voyatzakis, M. Amman, and K. Papailiou, "Optimum conductor arrangement of compact lines for electric and magnetic field minimization — Calculations and measurements," *Med Power*, Athens, Nov. 4–6, 2002.
14. Mimos, E. I., D. K. Tsanakas, and A. E. Tzinevrakis, "Solutions for high voltage transmission in suburban regions regarding the electric and magnetic fields," *Automation Congress*, 1–6, 2008.
15. Nunchuen, S. and V. Tarateeraseth, "Electric and magnetic field minimization using optimal phase arrangement techniques for MEA overhead power transmission lines," *ECTI Trans. Electr. Eng. Electron. Commun.*, Vol. 19, No. 1, 51–58, 2021.
16. Bansal, J. C., "Particle swarm optimization," *Studies in Computational Intelligence*, Vol. 779, 2019.
17. Katoch, S., S. S. Chauhan, and V. Kumar, "A review on genetic algorithm: Past, present, and future," *Multimedia Tools and Applications*, Vol. 80, No. 5, 8091–8126, 2021.
18. Kumar, M., M. Husain, N. Upreti, and D. Gupta, "Genetic algorithm: Review and application," *SSRN Electronic Journal*, 2020.

19. Al Salameh, M. S. H., I. M. Nejdawi, and O. A. Alani, "Using the nonlinear particle swarm optimization (PSO) algorithm to reduce the magnetic fields from overhead high voltage transmission lines," *Int. J. Res. Rev. Appl. Sci.*, Vol. 4, No. 1, 18–31, 2010.
20. Al Salameh M. S. H. and M. A. S. Hassouna, "Arranging overhead power transmission line conductors using swarm intelligence technique to minimize electromagnetic fields," *Progress In Electromagnetics Research B*, Vol. 26, 213–236, 2010.
21. El Dein, A. Z., "Optimal arrangement of egyptian overhead transmission lines' conductors using genetic algorithm," *Arabian Journal for Science & Engineering*, Vol. 39, No. 2, 1049–1059, 2014.
22. Deželak, K., F. Jakl, and G. Štumberger, "Arrangements of overhead power line phase conductors obtained by differential evolution," *Electr. Power Syst. Res.*, Vol. 81, No. 12, 2164–2170, Dec. 2011.
23. Paganotti, A. L., M. M. Afonso, M. A. de O. Schoeder, R. S. Alipio, and E. N. Gonçalves, "Arrangements of overhead power line phase conductors achieved by differential evolution method," *Sociedade Brasileira de Automática*, Vol. 1, No. 1, 2019.
24. Bravo-Rodríguez, J. C., J. C. Del-Pino-López, and P. Cruz-Romero, "A survey on optimization techniques applied to magnetic field mitigation in power systems," *Energies*, Vol. 12, No. 7, 1332, 2019.
25. Mirjalili, S., "The ant lion optimizer," *Adv. Eng. Softw.*, Vol. 83, 80–98, 2015.
26. Bayliss, C. R. and B. J. Hardy, *Transmission and Distribution: Electrical Engineering*, 4th Edition, Elsevier Ltd., UK, Feb. 2012.
27. Garrido, C., A. F. Otero, and J. Cidras, "Low-frequency magnetic fields from electrical appliances and power lines," *IEEE Transactions on Power Delivery*, Vol. 18, No. 4, 1310–1319, Oct. 2003.
28. Saadat, H., *Power System Analysis*, 2nd Edition, McGraw Hill, USA, 2002.
29. Al Hazaimeh, L. B., "Genetic algorithm optimization of the parameters of high voltage power transmission lines based on the emitted electromagnetic fields," M.Sc Thesis, Department of Electrical Engineering, Jordan University of Science and Technology, 2021.
30. Trlep, M., A. Hamler, M. Jesenik, and B. Stumberger, "Electric field distribution under transmission lines dependent on ground surface," *IEEE Transactions on Magnetics*, Vol. 45, No. 3, 1748–1751, 2009.
31. Winterfeldt, D., "Power grid and land use policy analysis," Final Report, California Department of Health Services, and the Public Health Institute, 2001.
32. Al Salameh, M. S. H., *Waves and Fields of Wireless Communications and Electricity: Health-effects and Unconventional Utilizations*, Lap Publishing, Printed in USA and in the UK, 2011.
33. Viscusi, W. K. and C. J. Masterman, "Income elasticities and global values of a statistical life," *Journal of Benefit-Cost Analysis*, Vol. 8, No. 2, 226–250, 2017.
34. Robinson, L. A., J. R. Baxter, and W. Raich, "2016 Guidelines for Regulatory Impact Analysis, Appendix D: Updating value per statistical life (VSL) estimates for inflation and changes in real income," U.S. Department of Health and Human Services, 2016.
35. United States General Accounting Office, "Electromagnetic fields: Federal efforts to determine health effects are behind schedule," Report to Committee on Natural Resources, House of Representatives, Washington, Jun. 1994, URL: https://www.gao.gov/assets/rced-94-115.pdf.
36. Website, World Bank data, "Inflation, consumer prices (annual %) — Jordan," https://data.worldbank.org/indicator/FP.CPI.TOTL.ZG?end=2020&locations=JO&start=1970 &view=chart.